$H \to ZZ^*$, $H \to \gamma\gamma$, $H \to WW^*$
Coupling measurements and interpretations at the ATLAS experiment

Davide Mungo
on behalf of the ATLAS Collaboration

University of Toronto

7 July 2022

Run1

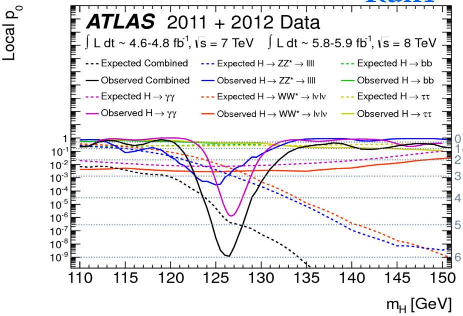

$H \to ZZ^*$, $H \to \gamma\gamma$, $H \to WW^*$

10y ago	First **observation** of Higgs boson production in Run1
∼today	Excellent **precision measurement** for Higgs boson properties
∼tomorrow	Run3 just officially started → **exciting times ahead!**

Presented here will be the **latest Run2** coupling analyses from ATLAS:

- $H \to ZZ^*$ (2020) HIGG-2018-28 published on EPJC
- $H \to \gamma\gamma$ (2022) **NEW** HIGG-2020-16 submitted to JHEP
- ggH/VBF $H \to WW^*$ (2022) **NEW** HIGG-2021-20 submitted to PRD

Other interesting ATLAS coupling measurements and EFT results today

$H \to ff$ coupling	H coupling combination	EFT interpretation	Analysis methods
Giulia and Robert	Zirui	Sandra	Stephen

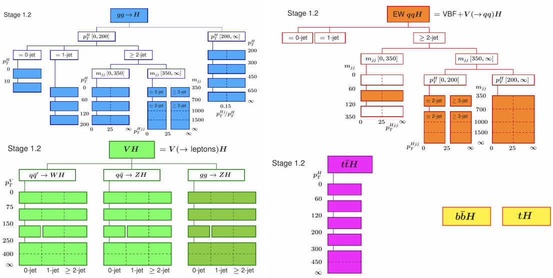

Established framework for
Higgs coupling measurement

STXS: Simplified Template X-Sections

- Measure production cross sections in **well-defined fiducial regions**
- **Less model dependent** with respect to inclusive measurement
- Provide some sort of unfold of detector-level effects

Interpretations: Standard Model Effective Field Theory (SMEFT) or κ-framework (see backup)

- **Modify tensor structure** of the SM with dimension-6 operators $\mathcal{O}_i^6$

$$\mathcal{L}_{\text{SMEFT}} = \mathcal{L}_{\text{SM}} + \sum_i \frac{c_i^{(6)}}{\Lambda^2}\mathcal{O}_i^{(6)}$$

- Parametrize STXS bin cross sections in terms of the **Wilson coefficients c_i**

$$\sigma_{\text{SMEFT}} \propto |\mathcal{M}_{\text{SMEFT}}|^2 =$$
$$= |\mathcal{M}_{\text{SM}}|^2 + \sum_i 2\text{Re}\left(\mathcal{M}_{\text{SM}}^*\mathcal{M}_i\right)\frac{c_i}{\Lambda^2} + \sum_{ij} 2\text{Re}\left(\mathcal{M}_i^*\mathcal{M}_i\right)\frac{c_i c_j}{\Lambda^4}$$
$$\propto \sigma_{SM}^{\text{STXS}}\left(1 + \sum_i A_i c_i + \sum_{ij} B_{ij} c_i c_j\right)$$

General analysis design

(Example from $H \to ZZ^* \to 4\ell$ analysis)

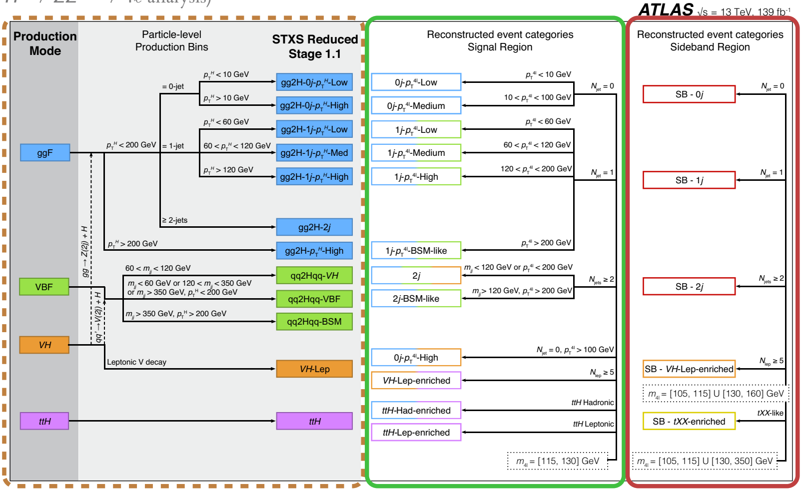

Reduced STXS target binning
- based on expected sensitivity

Analysis signal regions
- match STXS selections

Control regions
- constrain bkgs

$H \to 4\ell$ ANALYSIS STRATEGY

Main characteristics:

- **Higgs decay fully reconstructed**, access to Higgs kinematic
- Clean final state and excellent peak resolution
- High S/B ratio but mostly **limited** by signal **statistic**

Strategy: fit various NN binned outputs

Event selection:

- Two same-flavor opposite-charged lepton pairs (e, μ)
- Signal region $115 < m_{4\ell} < 130$ GeV, sideband for background constraint

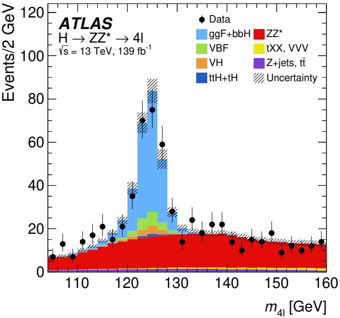

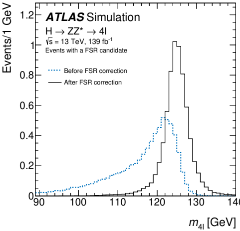

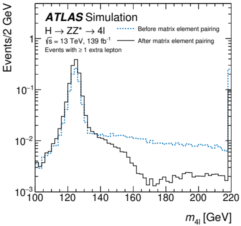

Improve $m_{4\ell}$ reconstruction

- Recovering FSR photons
- If > 4 leptons, selected quadruplet with ME discriminant
  - important for VH and ttH production modes

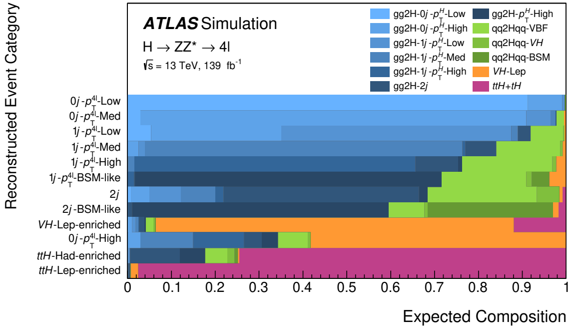

Dedicated NN trained for almost all categories

- NN combines an "event" NN + up to 2 "objects" RNNs (for leptons or for jets)
- NN output discriminates between two or three processes
  - examples: ggF-vs-ZZ or ggF-vs-VBF-vs-ZZ
- **Bin boundaries** chosen to **maximize significance**

Preselection using mostly rectangular cuts

- N_{jets}, $p_T^{4\ell}$, m_{jj} **following STXS bin boundaries**
- event selection starting from low cross sections production modes

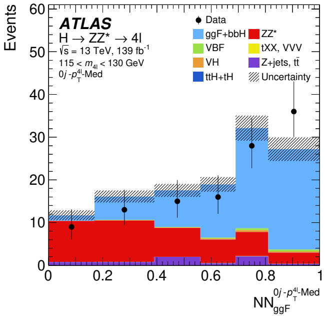

Main characteristics:

- **Higgs decay fully reconstructed**, access to Higgs kinematics
- Clean final state and excellent resolution
- **Larger background** compared to $H \to 4\ell$
  - but **robust data-driven subtraction**

Strategy: fit $m_{\gamma\gamma}$ shape and normalization

- Fully **analytical** signal+background **model**

Event selection:

- 2 well reconstructed and identified photons
- Signal region $105 < m_{\gamma\gamma} < 160$ GeV

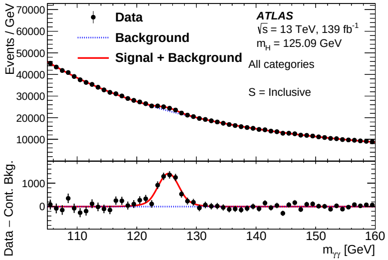

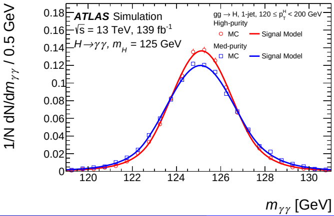

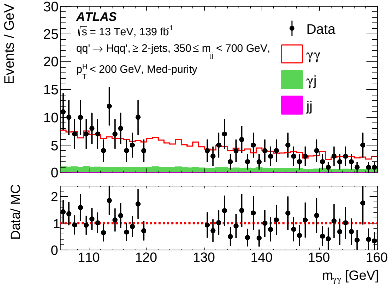

Unified optimization technique targeting
almost full STXS 1.2 scheme (45 bins) **simultaneously**

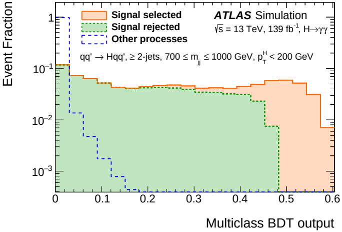

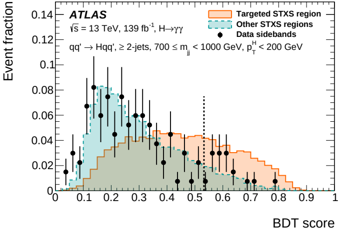

- **Multiclass BDT** to separate STXS signal bins
- **Weight** multiclass 45 **outputs** to optimize $|C_{\mathrm{STXS}}|$ of the STXS measurement
- "S-vs-B" **binary BDTs** for each region to reject bkg
  - additional NN for ***tHjb*** to separate $\kappa_t = \pm 1$ signals

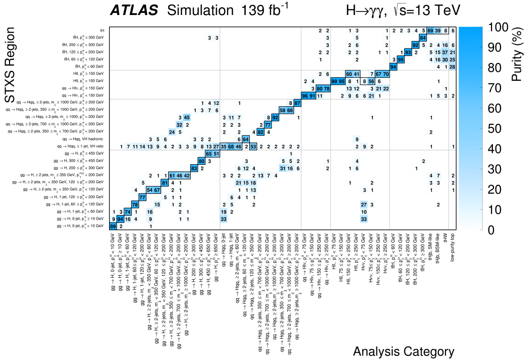

Main characteristics:

- Worse resolution due to 2ν, but **high signal yield**
- **Complex set of backgrounds** with large uncertainties

Strategy: target only ggH and VBF

- ggH regions: fit m_T observable
- VBF regions: fit DNN discriminant output

Event selection:

Two leptons different-flavor opposite-charged

- exploit **small opening angle between signal leptons** to suppress WW bkg

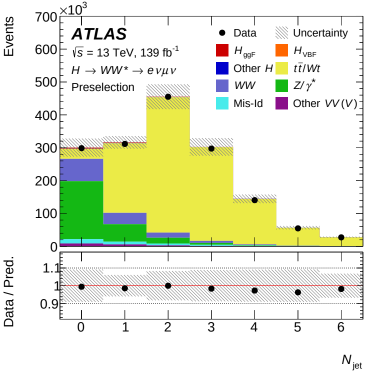

Specific selections for each N_{jet} analysis category, **different background** compositions

- $N_{jets} = 0$, $N_{jets} = 1$, $N_{jets} \geq 2$ (ggH), $N_{jets} \geq 2$ (VBF)

Cut based selection to reduce dominant backgrounds

- invert/additional selections to create specific CRs
- targeted WW, top, Z/γ^*

$ggH/VBF\ H \to WW^* \to e\nu\mu\nu$ CATEGORIZATION

JUST RELEASED!

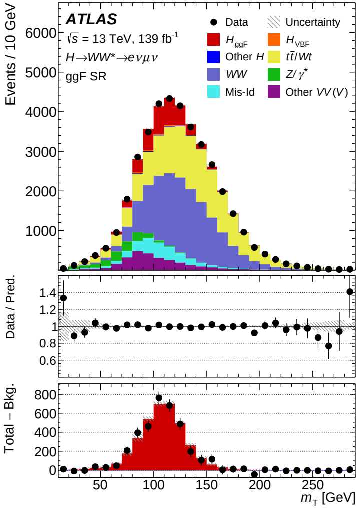

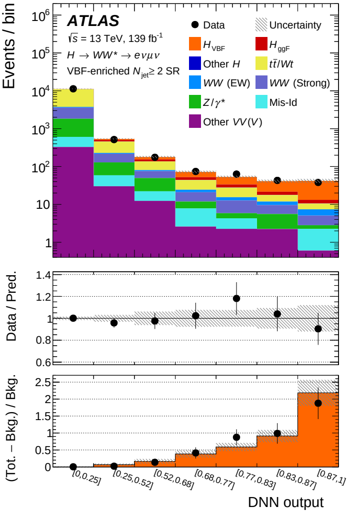

Final selections optimized for different measurement scheme

- inclusive ggF/VBF cross sections: ggF sub-regions split in $m_{\ell\ell}$ and $p_{\mathrm{T}}^{\text{sublead-}\ell}$
- STXS measurement: sub-regions in $p_{\mathrm{T}}^{H} \sim p_{\mathrm{T}}^{\ell\ell E_{\mathrm{T}}^{miss}}$ and m_{jj}
- VBF DNN bin boundaries are optimized in both cases

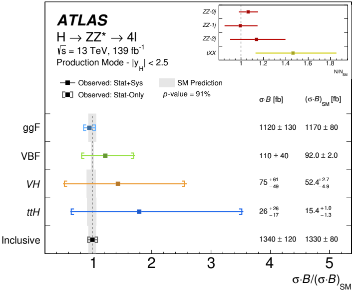

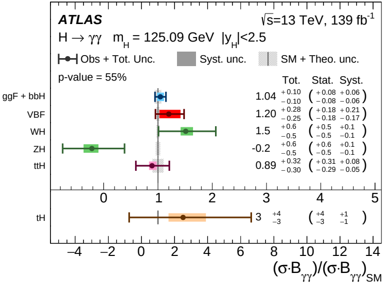

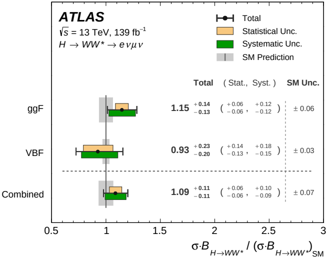

Good agreement with SM predictions so far

- $\sim 10\%$ relative uncertainty on **inclusive** measurement for all the channels
- $H \to ZZ^*$ stat-limited, $H \to WW^*$ syst-limited
- ggH known at $\sim 10\%$, VBF at $\lesssim 30\%$
- $\boldsymbol{\sigma_{\mathrm{tH}}^{\gamma\gamma}} < 10(6.8) \times \boldsymbol{\sigma_{\mathrm{SM}}}$ at 95% CL
  - $H \to \gamma\gamma$ **excludes negative κ_t at 2.2σ**
  - in case of unresolved loop (see backup)

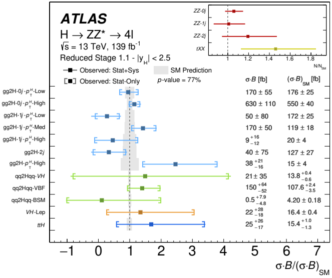
ATLAS
H → ZZ* → 4l
√s = 13 TeV, 139 fb^-1
Reduced Stage 1.1 - |y_H| < 2.5
Observed: Stat+Sys
Observed: Stat-Only
SM Prediction
p-value = 77%
σ·B [fb]
(σ·B)_SM [fb]
gg2H-0j-p_T^H-Low 170 ± 55 176 ± 25
gg2H-0j-p_T^H-High 630 ± 110 550 ± 40
gg2H-1j-p_T^H-Low 50 ± 80 172 ± 25
gg2H-1j-p_T^H-Med 170 ± 50 119 ± 18
gg2H-1j-p_T^H-High 9 +16 −12 20 ± 4
gg2H-2j 40 ± 75 127 ± 27
gg2H-p_T^H-High 38 +21 −16 15 ± 4
qq2Hqq-VH 21 ± 35 13.8 +0.4 −0.6
qq2Hqq-VBF 150 +64 −52 107.6 +2.4 −3.5
qq2Hqq-BSM 0.5 +7.9 −4.8 4.20 ± 0.18
VH-Lep 22 +28 −18 16.4 ± 0.4
ttH 25 +26 −17 15.4 +1.0 −1.3
ZZ-0j
ZZ-1j
ZZ-2j
tXX
N/N_SM
σ·B/(σ·B)_SM

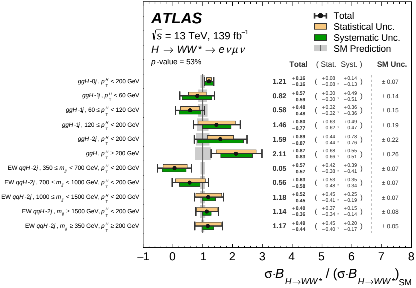
ATLAS
√s = 13 TeV, 139 fb^-1
H → WW* → eνμν
p-value = 53%
Total
Statistical Unc.
Systematic Unc.
SM Prediction
Total (Stat. Syst.) SM Unc.
ggH-0j, p_T^H < 200 GeV 1.21 +0.16 −0.16 (+0.08 −0.08, +0.14 −0.13) ± 0.07
ggH-1j, p_T^H < 60 GeV 0.82 +0.57 −0.59 (+0.30 −0.30, +0.49 −0.51) ± 0.14
ggH-1j, 60 ≤ p_T^H < 120 GeV 0.58 +0.48 −0.48 (+0.32 −0.32, +0.36 −0.36) ± 0.15
ggH-1j, 120 ≤ p_T^H < 200 GeV 1.46 +0.80 −0.77 (+0.63 −0.62, +0.49 −0.47) ± 0.19
ggH-2j, p_T^H < 200 GeV 1.59 +0.89 −0.87 (+0.44 −0.44, +0.78 −0.76) ± 0.22
ggH, p_T^H ≥ 200 GeV 2.11 +0.87 −0.83 (+0.68 −0.66, +0.55 −0.51) ± 0.26
EW qqH-2j, 350 ≤ m_jj < 700 GeV, p_T^H < 200 GeV 0.05 +0.57 −0.57 (+0.42 −0.38, +0.39 −0.41) ± 0.07
EW qqH-2j, 700 ≤ m_jj < 1000 GeV, p_T^H < 200 GeV 0.56 +0.63 −0.58 (+0.53 −0.48, +0.35 −0.34) ± 0.07
EW qqH-2j, 1000 ≤ m_jj < 1500 GeV, p_T^H < 200 GeV 1.18 +0.52 −0.45 (+0.45 −0.41, +0.25 −0.19) ± 0.07
EW qqH-2j, m_jj ≥ 1500 GeV, p_T^H < 200 GeV 1.14 +0.40 −0.36 (+0.37 −0.34, +0.15 −0.14) ± 0.08
EW qqH-2j, m_jj ≥ 350 GeV, p_T^H ≥ 200 GeV 1.17 +0.49 −0.44 (+0.45 −0.40, +0.20 −0.17) ± 0.05
σ·B_H→WW* / (σ·B_H→WW*)_SM

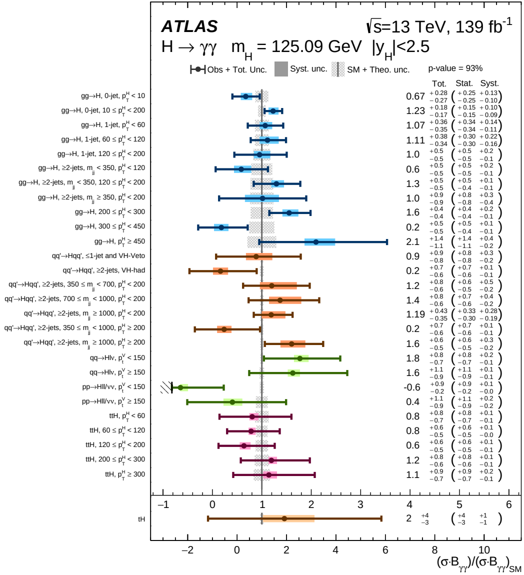
ATLAS
√s=13 TeV, 139 fb^-1
H → γγ m_H = 125.09 GeV |y_H|<2.5
Obs + Tot. Unc.
Syst. unc.
SM + Theo. unc.
p-value = 93%
Tot. Stat. Syst.
gg→H, 0-jet, p_T^H < 10 0.67
gg→H, 0-jet, 10 ≤ p_T^H < 200 1.23
gg→H, 1-jet, p_T^H < 60 1.07
gg→H, 1-jet, 60 ≤ p_T^H < 120 1.11
gg→H, 1-jet, 120 ≤ p_T^H < 200 1.0
gg→H, ≥2-jets, m_jj < 350, p_T^H < 120 0.6
gg→H, ≥2-jets, m_jj < 350, 120 ≤ p_T^H < 200 1.3
gg→H, ≥2-jets, m_jj ≥ 350, p_T^H < 200 1.0
gg→H, 200 ≤ p_T^H < 300 1.6
gg→H, 300 ≤ p_T^H < 450 0.2
gg→H, p_T^H ≥ 450 2.1
qq'→Hqq', ≤1-jet and VH-Veto 0.9
qq'→Hqq', ≥2-jets, VH-had 0.2
qq'→Hqq', ≥2-jets, 350 ≤ m_jj < 700, p_T^H < 200 1.2
qq'→Hqq', ≥2-jets, 700 ≤ m_jj < 1000, p_T^H < 200 1.4
qq'→Hqq', ≥2-jets, m_jj ≥ 1000, p_T^H < 200 1.19
qq'→Hqq', ≥2-jets, 350 ≤ m_jj < 1000, p_T^H ≥ 200 0.2
qq'→Hqq', ≥2-jets, m_jj ≥ 1000, p_T^H ≥ 200 1.6
qq→Hlν, p_T^V < 150 1.8
qq→Hlν, p_T^V ≥ 150 1.6
pp→Hll/νν, p_T^V < 150 -0.6
pp→Hll/νν, p_T^V ≥ 150 0.4
ttH, p_T^H < 60 0.8
ttH, 60 ≤ p_T^H < 120 0.8
ttH, 120 ≤ p_T^H < 200 0.6
ttH, 200 ≤ p_T^H < 300 1.2
ttH, p_T^H ≥ 300 1.1
tH 2 +4 −3
(σ·B_γγ)/(σ·B_γγ)_SM

EFT interpretation carried out in $H \to ZZ^*$ and $H \to \gamma\gamma$ channels

- Considered both linear and quadratic modification terms to the cross section

Both channels provide results with one Wilson coefficient varied at a time. Moreover

- $H \to ZZ^*$ **simultaneous** variation of **two coefficients** (see backup)
- $H \to \gamma\gamma$ **full simultaneous fit**, via PCA

$H \to ZZ^*$ EFT interpretation: test 10 different operators

Important analysis acceptance corrections

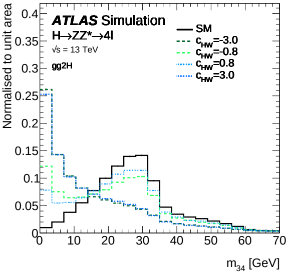

CP-even operators

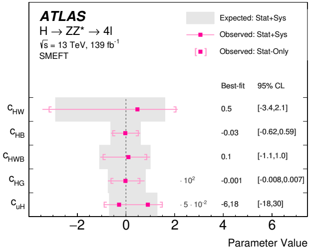

CP-odd operators

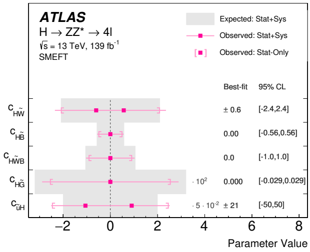

Single c_i results compatible with SM

Tested **34 different operators**

- not enough information in STXS measurement to constrain each of them
- multiple operators contribute to same STXS bin

$\Rightarrow$ **Principal Component Analysis**

- Identify eigenvectors of $C_{\text{SMEFT}}^{-1} = P^T C_{\text{STXS}}^{-1} P$
- **Align** measurement **parameters to eigenvectors**
- Perform fit to not-flat directions only
  - 12 directions remaining ($\lambda_n > 0.005$)

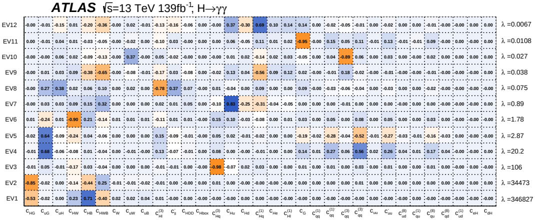

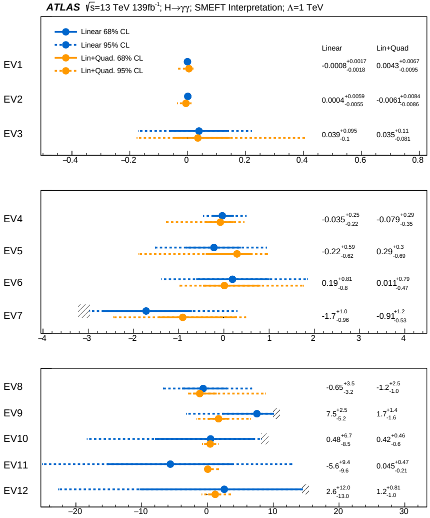

After 10 years, $H \to ZZ^*$, $H \to \gamma\gamma$, $H \to WW^*$ continue to provide great insights into Higgs boson production

- Presented **latest Run 2 results** for production mode and STXS cross sections measurements
- All presented measurements show **good agreement with the SM** expectation
  - Inclusive cross section known at 10%, ggF at 10% and VBF at $\lesssim 30\%$
  - ggH/VBF STXS bins measured at $\lesssim 50\%$, differential ttH in $H \to \gamma\gamma$
  - Excluded negative κ_t at 2.2σ directly from tH
- Performed SM Effective Field Theory **interpretation, no signs of deviation observed**
- Most of the measurements presented are still **statistically limited**

Looking at future, the Run3 dataset will still be a joyful playground for these channels

Backup

Consistent treatment of production and decay processes $\Rightarrow$ **$\boldsymbol{\kappa}$ modifiers**

Basic assumptions:

- **No additional Higgs boson decays beyond SM**
- **Narrow width** approximation $\Rightarrow$ decoupling of production and decay processes

$$\sigma_i \times \mathrm{BR}^f = \frac{\sigma_i(\boldsymbol{\kappa}) \times \Gamma^f(\boldsymbol{\kappa})}{\Gamma_H}$$

with κ defined as

$$\kappa_j^2 = \frac{\sigma_j}{\sigma_j^{\mathrm{SM}}} \quad \text{or} \quad \kappa_j^2 = \frac{\Gamma_j}{\Gamma_j^{\mathrm{SM}}}$$

Best available SM predictions when all $\kappa_i = 1$, high order accuracy lost when $\kappa_i \neq 1$

For loop processes ggH and $H \to \gamma\gamma$ two possibilities:

- **effective** couplings κ_g and κ_γ
- **resolved** parametrization with κ_t, κ_b and κ_W

The **ggZH loop** is always treated as **resolved**

$H \to ZZ^*$

List of different variables for NN: $H \to ZZ^*$

Category	Processes	MLP	Lepton RNN	Jet RNN	Discriminant
$0j$-$p_T^{4\ell}$-Low $0j$-$p_T^{4\ell}$-Med	ggF, ZZ^*	$p_T^{4\ell}$, D_{ZZ^*}, m_{12}, m_{34}, $\lvert\cos\theta^*\rvert$, $\cos\theta_1$, ϕ_{ZZ}	p_T^ℓ, η_ℓ	-	NN_{ggF}
$1j$-$p_T^{4\ell}$-Low	ggF, VBF, ZZ^*	$p_T^{4\ell}$, p_T^j, η_j, $\Delta R_{4\ell j}$, D_{ZZ^*}	p_T^ℓ, η_ℓ	-	NN_{VBF} for $NN_{ZZ} < 0.25$ NN_{ZZ} for $NN_{ZZ} > 0.25$
$1j$-$p_T^{4\ell}$-Med	ggF, VBF, ZZ^*	$p_T^{4\ell}$, p_T^j, η_j, E_T^{miss}, $\Delta R_{4\ell j}$, D_{ZZ^*}, $\eta_{4\ell}$	p_T^ℓ, η_ℓ	-	NN_{VBF} for $NN_{ZZ} < 0.25$ NN_{ZZ} for $NN_{ZZ} > 0.25$
$1j$-$p_T^{4\ell}$-High	ggF, VBF	$p_T^{4\ell}$, p_T^j, η_j, E_T^{miss}, $\Delta R_{4\ell j}$, $\eta_{4\ell}$	p_T^ℓ, η_ℓ	-	NN_{VBF}
$2j$	ggF, VBF, VH	m_{jj}, $p_T^{4\ell jj}$	p_T^ℓ, η_ℓ	p_T^j, η_j	NN_{VBF} for $NN_{VH} < 0.2$ NN_{VH} for $NN_{VH} > 0.2$
$2j$-BSM-like	ggF, VBF	η_{ZZ}^{Zepp}, $p_T^{4\ell jj}$	p_T^ℓ, η_ℓ	p_T^j, η_j	NN_{VBF}
VH-Lep-enriched	VH, ttH	N_{jets}, $N_{b\text{-jets},70\%}$, E_T^{miss}, H_T	p_T^ℓ	-	NN_{ttH}
ttH-Had-enriched	ggF, ttH, tXX	$p_T^{4\ell}$, m_{jj}, $\Delta R_{4\ell j}$, $N_{b\text{-jets},70\%}$,	p_T^ℓ, η_ℓ	p_T^j, η_j	NN_{ttH} for $NN_{tXX} < 0.4$ NN_{tXX} for $NN_{tXX} > 0.4$

Measurement	Experimental uncertainties [%]				Theory uncertainties [%]				
	Lumi.	e, μ, pile-up	Jets, flav. tag	Reducible bkg	Background ZZ^*	Background tXX	Signal PDF	Signal QCD	Signal Shower
Inclusive cross-section									
	1.7	2.5	0.5	< 0.5	1	< 0.5	< 0.5	1	2
Production mode cross-sections									
ggF	1.7	2.5	1	< 0.5	1.5	< 0.5	0.5	1	2
VBF	1.7	2	4	< 0.5	1.5	< 0.5	1	5	7
VH	1.9	2	4	1	6	< 0.5	2	13.5	7.5
ttH	1.7	2	6	< 0.5	1	0.5	0.5	12.5	4
Reduced Stage-1.1 production bin cross-sections									
gg2H-0j-p_T^H-Low	1.7	3	1.5	0.5	6.5	< 0.5	< 0.5	1	1.5
gg2H-0j-p_T^H-High	1.7	3	5	< 0.5	3	< 0.5	< 0.5	0.5	5.5
gg2H-1j-p_T^H-Low	1.7	2.5	12	0.5	7	< 0.5	< 0.5	1	6
gg2H-1j-p_T^H-Med	1.7	3	7.5	< 0.5	1	< 0.5	< 0.5	1.5	5.5
gg2H-1j-p_T^H-High	1.7	3	11	0.5	2	< 0.5	< 0.5	2	7.5
gg2H-2j	1.7	2.5	16.5	1	12.5	0.5	< 0.5	2.5	10.5
gg2H-p_T^H-High	1.7	1.5	3	0.5	3.5	< 0.5	< 0.5	2	3.5
qq2Hqq-VH	1.8	4	17	1	4	1	0.5	5.5	8
qq2Hqq-VBF	1.7	2	3.5	< 0.5	5	< 0.5	< 0.5	6	10.5
qq2Hqq-BSM	1.7	2	4	< 0.5	2.5	< 0.5	< 0.5	3	8
VH-Lep	1.8	2.5	2	1	2	0.5	< 0.5	1.5	3
ttH	1.7	2.5	5	0.5	1	0.5	< 0.5	11	3

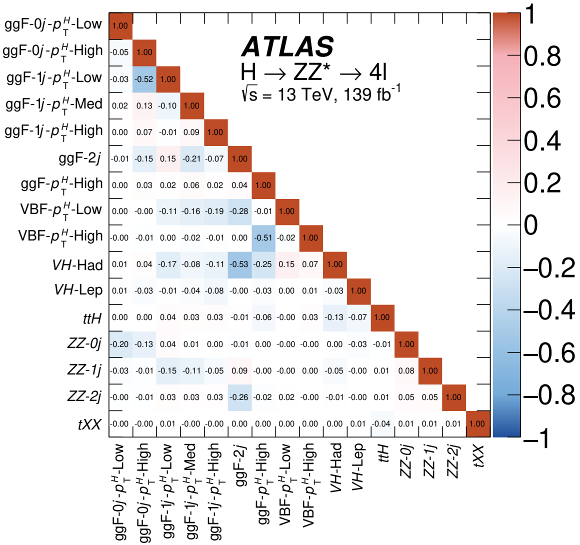
ATLAS
H → ZZ* → 4l
√s = 13 TeV, 139 fb-1
ggF-0j-pT^H-Low 1.00
ggF-0j-pT^H-High -0.05 1.00
ggF-1j-pT^H-Low -0.03 -0.52 1.00
ggF-1j-pT^H-Med 0.02 0.13 -0.10 1.00
ggF-1j-pT^H-High 0.00 0.07 -0.01 0.09 1.00
ggF-2j -0.01 -0.15 0.15 -0.21 -0.07 1.00
ggF-pT^H-High 0.00 0.03 0.02 0.06 0.02 0.04 1.00
VBF-pT^H-Low 0.00 -0.00 -0.11 -0.16 -0.19 -0.28 -0.01 1.00
VBF-pT^H-High -0.00 -0.01 0.00 -0.02 -0.01 0.00 -0.51 -0.02 1.00
VH-Had 0.01 0.04 -0.17 -0.08 -0.11 -0.53 -0.25 0.15 0.07 1.00
VH-Lep 0.01 -0.03 -0.01 -0.04 -0.08 -0.00 -0.03 0.00 0.01 -0.03 1.00
ttH 0.00 0.00 0.04 0.03 0.03 -0.01 -0.06 -0.00 0.03 -0.13 -0.07 1.00
ZZ-0j -0.20 -0.13 0.04 0.01 0.00 -0.01 0.00 -0.00 -0.00 0.00 -0.03 -0.01 1.00
ZZ-1j -0.03 -0.01 -0.15 -0.11 -0.05 0.09 -0.00 -0.00 0.00 -0.05 -0.00 0.01 0.08 1.00
ZZ-2j -0.00 -0.01 0.03 0.03 0.03 -0.26 -0.02 0.02 -0.00 -0.01 -0.00 0.01 0.05 0.05 1.00
tXX -0.00 -0.00 0.01 -0.00 -0.00 0.00 0.00 0.00 0.00 0.00 0.01 -0.04 0.01 0.01 0.01 1.00
ggF-0j-pT^H-Low ggF-0j-pT^H-High ggF-1j-pT^H-Low ggF-1j-pT^H-Med ggF-1j-pT^H-High ggF-2j ggF-pT^H-High VBF-pT^H-Low VBF-pT^H-High VH-Had VH-Lep ttH ZZ-0j ZZ-1j ZZ-2j tXX
1
0.8
0.6
0.4
0.2
0
−0.2
−0.4
−0.6
−0.8
−1

The expected impact of the CP-odd and CP-even Wilson coefficients on the cross section of the STXS bins

- chosen value of the Wilson coefficient corresponds almost to the expected 68% CL
- black points are the observed values of the STXS measurements

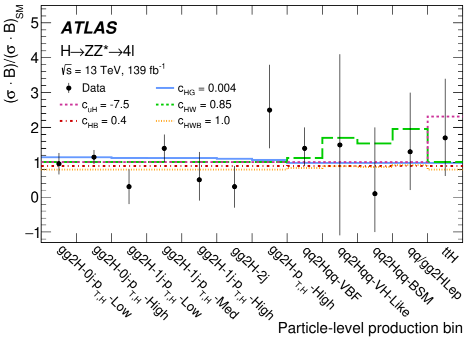

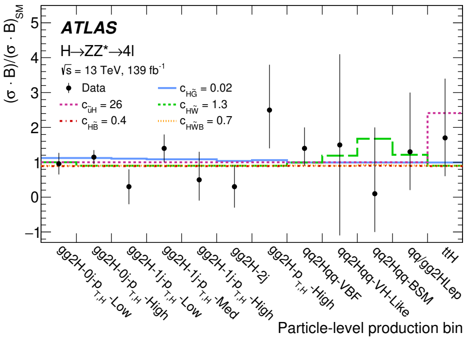

EFT interpretation

Performed interpretation with two Wilson coefficients simultaneously fitted

- other coefficients fixed to 0

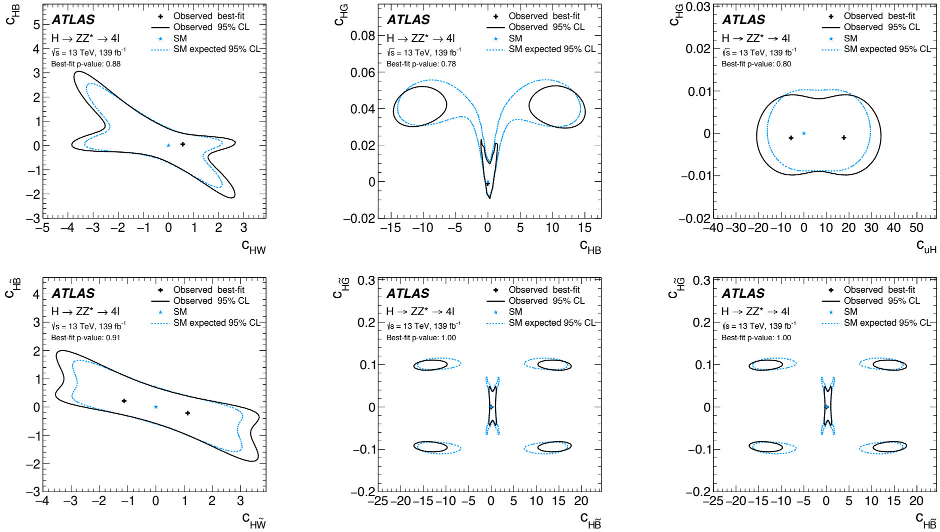

$H \to \gamma\gamma$

Multiclass BDT

$\eta_{\gamma_1}, \eta_{\gamma_2}, p_{\mathrm{T}}^{\gamma\gamma}, y_{\gamma\gamma}$, $p_{\mathrm{T},jj}^{\dagger}$, m_{jj}, and Δy, $\Delta\phi$, $\Delta\eta$ between j_1 and j_2, $p_{\mathrm{T},\gamma\gamma j_1}, m_{\gamma\gamma j_1}, p_{\mathrm{T},\gamma\gamma jj}\dagger, m_{\gamma\gamma jj}$ Δy, $\Delta\phi$ between the $\gamma\gamma$ and jj systems, minimum ΔR between jets and photons, invariant mass of the system comprising all jets in the event, dilepton p_{T}, di-e or di-μ invariant mass (leptons are required to be oppositely charged), $E_{\mathrm{T}}^{\mathrm{miss}}$, p_{T} and transverse mass of the lepton + $E_{\mathrm{T}}^{\mathrm{miss}}$ system, p_{T}, η, ϕ of top-quark candidates, $m_{t_1 t_2}$ Number of jets†, of central jets ($\lvert\eta\rvert < 2.5$)†, of b-jets† and of leptons, p_{T} of the highest-p_{T} jet, scalar sum of the p_{T} of all jets, scalar sum of the transverse energies of all particles ($\sum E_{\mathrm{T}}$), $E_{\mathrm{T}}^{\mathrm{miss}}$ significance, $\left\lvert E_{\mathrm{T}}^{\mathrm{miss}} - E_{\mathrm{T}}^{\mathrm{miss}}(\text{primary vertex with the highest } \sum p_{\mathrm{T,track}}^2)\right\rvert > 30\,\mathrm{GeV}$ Top reconstruction BDT of the top-quark candidates, $\Delta R(W, b)$ of t_2, $\eta_{j_F}, m_{\gamma\gamma j_F}$ Average number of interactions per bunch crossing.

Binary BDTs

STXS classes	Variables
Individual STXS classes from $gg \to H$ $qq' \to Hqq'$ $qq \to H\ell\nu$ $pp \to H\ell\ell$ $pp \to H\nu\bar{\nu}$	All multiclass BDT variables, $\boldsymbol{p}_{\mathrm{T}}^{\gamma\gamma}$ projected to the thrust axis of the $\gamma\gamma$ system ($p_{\mathrm{Tt}}^{\gamma\gamma}$), $\Delta\eta_{\gamma\gamma}, \eta^{\mathrm{Zepp}} = \frac{\eta_{\gamma\gamma}-\eta_{jj}}{2}$, $\phi_{\gamma\gamma}^{*} = \tan\left(\frac{\pi-\lvert\Delta\phi_{\gamma\gamma}\rvert}{2}\right)\sqrt{1-\tanh^2\left(\frac{\Delta\eta_{\gamma\gamma}}{2}\right)}$, $\cos\theta_{\gamma\gamma}^{*} = \left\lvert\frac{(E^{\gamma_1}+p_z^{\gamma_1})\cdot(E^{\gamma_2}-p_z^{\gamma_2})-(E^{\gamma_1}-p_z^{\gamma_1})\cdot(E^{\gamma_2}+p_z^{\gamma_2})}{m_{\gamma\gamma}+\sqrt{m_{\gamma\gamma}^2+(p_{\mathrm{T}}^{\gamma\gamma})^2}}\right\rvert$ Number of electrons and muons.
all $t\bar{t}H$ and tHW STXS classes combined	p_{T}, η, ϕ of γ_1 and γ_2, p_{T}, η, ϕ and b-tagging scores of the six highest-p_{T} jets, $E_{\mathrm{T}}^{\mathrm{miss}}$, $E_{\mathrm{T}}^{\mathrm{miss}}$ significance, $E_{\mathrm{T}}^{\mathrm{miss}}$ azimuthal angle, Top reconstruction BDT scores of the top-quark candidates, p_{T}, η, ϕ of the two highest-p_{T} leptons.
$tHqb$	$p_{\mathrm{T}}^{\gamma\gamma}/m_{\gamma\gamma}$, $\eta_{\gamma\gamma}$, p_{T}, invariant mass, BDT score and $\Delta R(W, b)$ of t_1, p_{T}, η of t_2, p_{T}, η of j_F, Angular variables: $\Delta\eta_{\gamma\gamma t_1}, \Delta\theta_{\gamma\gamma t_2}, \Delta\theta_{t_1 j_F}, \Delta\theta_{t_2 j_F}, \Delta\theta_{\gamma\gamma j_F}$ Invariant mass variables: $m_{\gamma\gamma j_F}, m_{t_1 j_F}, m_{t_2 j_F}, m_{\gamma\gamma t_1}$ Number of jets with $p_{\mathrm{T}} > 25\,\mathrm{GeV}$, Number of b-jets with $p_{\mathrm{T}} > 25\,\mathrm{GeV}^{*}$; Number of leptons*, $E_{\mathrm{T}}^{\mathrm{miss}}$ significance*

Category composition in terms of STXS signals

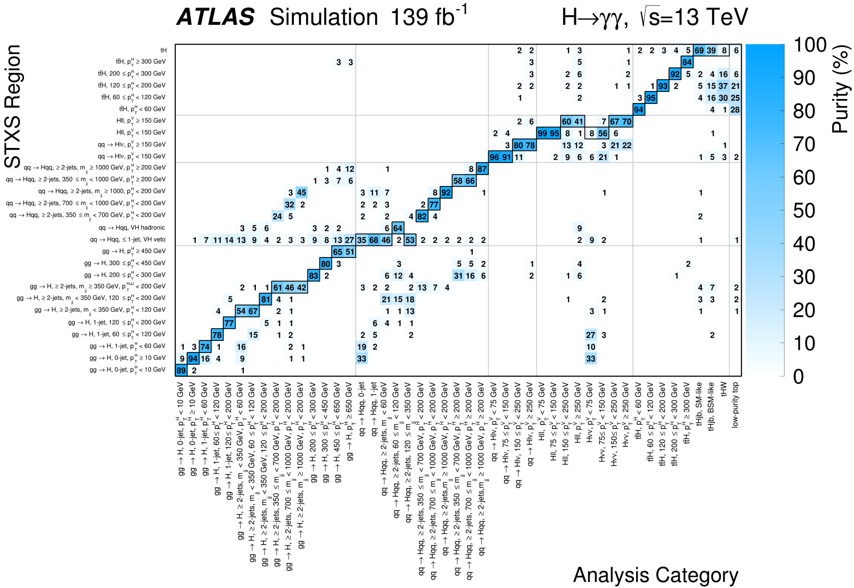

Dominant systematic uncertainties in $H \to \gamma\gamma$

	ggF + $b\bar{b}$H	VBF	WH	ZH	$t\bar{t}H$	tH
Uncertainty source	$\Delta\sigma[\%]$	$\Delta\sigma[\%]$	$\Delta\sigma[\%]$	$\Delta\sigma[\%]$	$\Delta\sigma[\%]$	$\Delta\sigma[\%]$
Theory uncertainties						
Higher-order QCD terms	±1.4	±4.1	±4.1	±12	±2.8	±16
Underlying event and parton shower	±2.5	±16	±2.5	±4.0	±3.6	±48
PDF and α_s	< ±1	±2.0	±1.4	±2.3	< ±1	±5.8
Matrix element	< ±1	±3.2	< ±1	±1.2	±2.5	±8.2
Heavy-flavour jet modelling in non-$t\bar{t}H$ processes	< ±1	< ±1	< ±1	< ±1	< ±1	±13
Experimental uncertainties						
Photon energy resolution	±3.0	±3.0	±3.8	±4.8	±3.0	±12
Photon efficiency	±2.7	±2.7	±3.3	±3.6	±2.9	±9.3
Luminosity	±1.8	±2.0	±2.4	±2.7	±2.2	±6.6
Pile-up	±1.4	±2.2	±2.0	±2.3	±1.4	±7.3
Background modelling	±2.0	±4.6	±3.6	±7.2	±2.5	±63
Photon energy scale	< ±1	< ±1	< ±1	±1.3	< ±1	±5.6
Jet/E_T^{miss}	< ±1	±6.8	< ±1	±2.2	±3.5	±22
Flavour tagging	< ±1	< ±1	< ±1	< ±1	±1.5	±3.4
Leptons	< ±1	< ±1	< ±1	< ±1	< ±1	±1.8
Higgs boson mass	< ±1	< ±1	< ±1	< ±1	< ±1	< ±1

Production mode

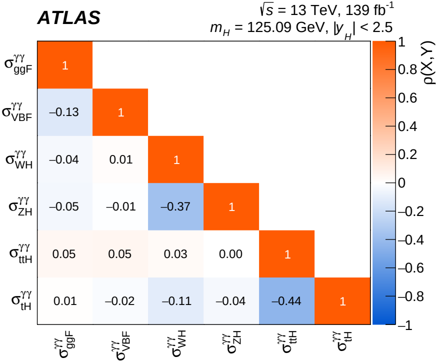

STXS

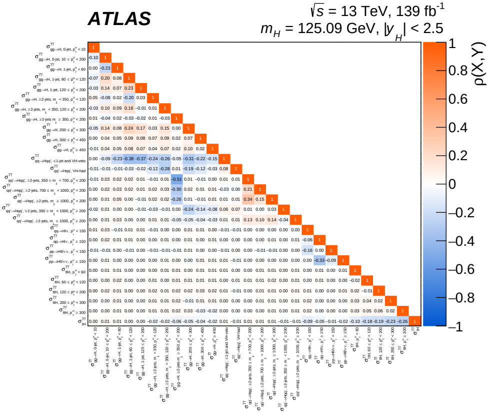

Four different models are considered, targeting different Higgs couplings

- value and sign of top-quark coupling

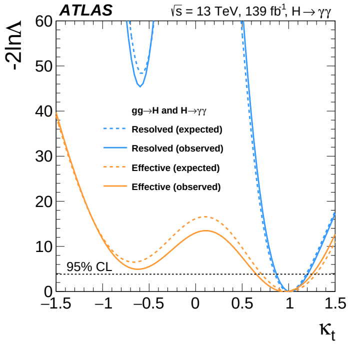

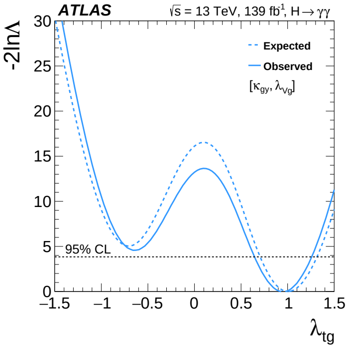

Direct test of top quark coupling

- other coupling fixed to SM
- $\kappa_t < 0$ excluded at $2.2\sigma(6.7\sigma)$ with effective(resolved) loop
  - sensitivity directly from tH prod mode

Generic parametrization with coupling ratios

- $\kappa_{g\gamma} = \frac{\kappa_g \kappa_\gamma}{\kappa_H}$, $\lambda_{Vg} = \frac{\kappa_V}{\kappa_g}$, $\lambda_{tg} = \frac{\kappa_t}{\kappa_g}$
- no assumptions on Higgs total width
- $\lambda_{tg} < 0$ excluded at 2.1σ

Four different models are considered, targeting different Higgs couplings

- presence of BSM physics in loop processes (κ_g, κ_γ)
- unified couplings to fermion and vector bosons (κ_V, κ_F)

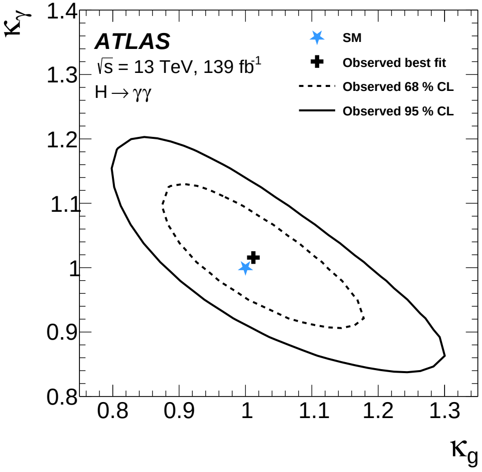

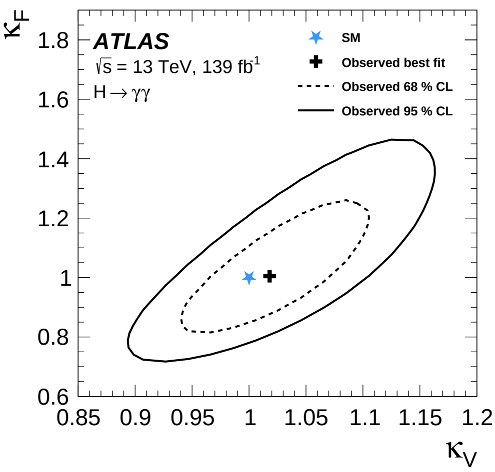

EFT interpretation in $H \to \gamma\gamma$

The expected impact of the most relevant EFT operators on the cross section of the STXS bins

- chosen value of the Wilson coefficient corresponds almost to the expected 68% CL
- $gg \to H$ and ttH (second), the $H \to \gamma\gamma$ decay (third), and VBF and VH processes (bottom)

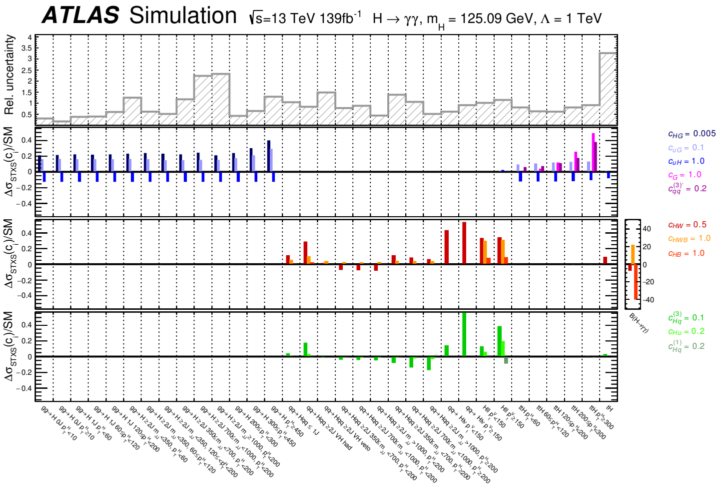

Individual EFT coefficients measurements in $H \to \gamma\gamma$

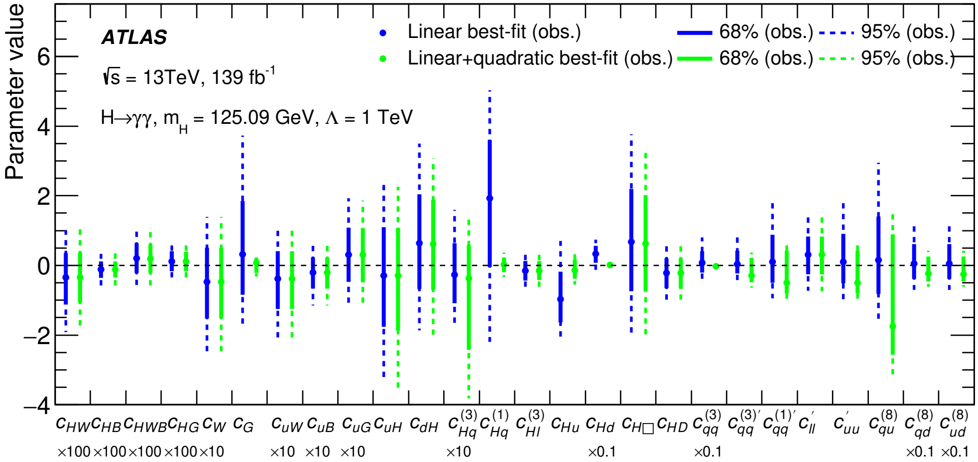

Expected correlations

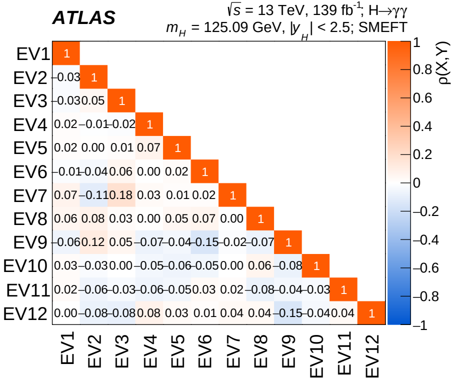

Observed correlations

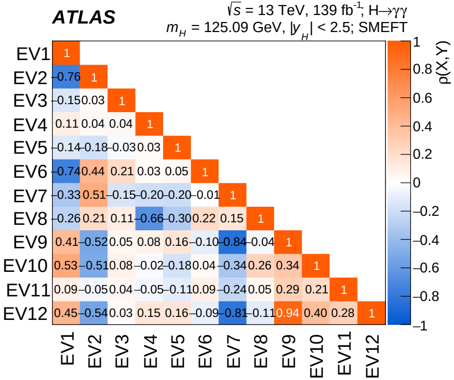

$H \to WW^*$

Preselection signal composition in $H \to WW^*$

<table>
<tr><th>Category</th><th>$N_{\text{jet},(p_T>30\text{ GeV})} = 0$ ggF</th><th>$N_{\text{jet},(p_T>30\text{ GeV})} = 1$ ggF</th><th>$N_{\text{jet},(p_T>30\text{ GeV})} \geq 2$ ggF</th><th>$N_{\text{jet},(p_T>30\text{ GeV})} \geq 2$ VBF</th></tr>
<tr><td rowspan="2">Preselection</td><td colspan="4">Two isolated, different-flavor leptons ($\ell = e, \mu$) with opposite charge
$p_T^{\text{lead}} > 22$ GeV , $p_T^{\text{sublead}} > 15$ GeV
$m_{\ell\ell} > 10$ GeV</td></tr>
<tr><td colspan="3">$p_T^{\text{miss}} > 20$ GeV</td><td></td></tr>
<tr><td rowspan="3">Background rejection</td><td colspan="4">$N_{b\text{-jet},(p_T>20\text{ GeV})} = 0$</td></tr>
<tr><td rowspan="2">$\Delta\phi_{\ell\ell,E_T^{\text{miss}}} > \pi/2$
$p_T^{\ell\ell} > 30$ GeV</td><td colspan="3">$m_{\tau\tau} < m_Z - 25$ GeV</td></tr>
<tr><td>max $(m_T^{\ell}) > 50$ GeV</td><td colspan="2"></td></tr>
<tr><td rowspan="3">$H \to WW^* \to e\nu\mu\nu$
topology</td><td colspan="3">$m_{\ell\ell} < 55$ GeV
$\Delta\phi_{\ell\ell} < 1.8$</td><td rowspan="3">central jet veto
outside lepton veto
$m_{jj} > 120$ GeV</td></tr>
<tr><td colspan="2" rowspan="2"></td><td>fail central jet veto
or
fail outside lepton veto</td></tr>
<tr><td>$|m_{jj} - 85| > 15$ GeV
or
$\Delta y_{jj} > 1.2$</td></tr>
<tr><td>Discriminating fit variable</td><td colspan="3">m_T</td><td>DNN</td></tr>
</table>

Control regions selection in $H \to WW^*$

<table>
<tr><th>CR</th><th>$N_{\text{jet},(p_T>30\text{ GeV})} = 0$ ggF</th><th>$N_{\text{jet},(p_T>30\text{ GeV})} = 1$ ggF</th><th>$N_{\text{jet},(p_T>30\text{ GeV})} \geq 2$ ggF</th><th>$N_{\text{jet},(p_T>30\text{ GeV})} \geq 2$ VBF</th></tr>
<tr><td rowspan="5">$qq \to WW$</td><td colspan="3">$N_{b\text{-jet},(p_T>20\text{ GeV})} = 0$</td><td rowspan="5"></td></tr>
<tr><td rowspan="4">$\Delta\phi_{\ell\ell,E_T^{miss}} > \pi/2$
$p_T^{\ell\ell} > 30$ GeV
$55 < m_{\ell\ell} < 110$ GeV
$\Delta\phi_{\ell\ell} < 2.6$</td><td colspan="2">$m_{\ell\ell} > 80$ GeV</td></tr>
<tr><td rowspan="3">$\lvert m_{\tau\tau} - m_Z\rvert > 25$ GeV
$\max\left(m_T^{\ell}\right) > 50$ GeV</td><td>$m_{\tau\tau} < m_Z - 25$ GeV
$m_{T2} > 165$ GeV</td></tr>
<tr><td>fail central jet veto
or fail outside lepton veto</td></tr>
<tr><td>$\lvert m_{jj} - 85\rvert > 15$ GeV
or $\Delta y_{jj} > 1.2$</td></tr>
<tr><td rowspan="5">$t\bar{t}/Wt$</td><td rowspan="5">$N_{b\text{-jet},(20<p_T<30\text{ GeV})} > 0$

$\Delta\phi_{\ell\ell,E_T^{miss}} > \pi/2$
$p_T^{\ell\ell} > 30$ GeV
$\Delta\phi_{\ell\ell} < 2.8$</td><td>$N_{b\text{-jet},(p_T>30\text{ GeV})} = 1$
$N_{b\text{-jet},(20<p_T<30\text{ GeV})} = 0$</td><td>$N_{b\text{-jet},(p_T>20\text{ GeV})} = 0$</td><td>$N_{b\text{-jet},(p_T>20\text{ GeV})} = 1$</td></tr>
<tr><td colspan="3">$m_{\tau\tau} < m_Z - 25$ GeV</td></tr>
<tr><td rowspan="3">$\max\left(m_T^{\ell}\right) > 50$ GeV</td><td>$m_{\ell\ell} > 80$ GeV
$\Delta\phi_{\ell\ell} < 1.8$
$m_{T2} < 165$ GeV</td><td rowspan="3">central jet veto
outside lepton veto</td></tr>
<tr><td>fail central jet veto
or fail outside lepton veto</td></tr>
<tr><td>$\lvert m_{jj} - 85\rvert > 15$ GeV
or $\Delta y_{jj} > 1.2$</td></tr>
<tr><td rowspan="5">Z/γ^*</td><td colspan="4">$N_{b\text{-jet},(p_T>20\text{ GeV})} = 0$</td></tr>
<tr><td colspan="2">$m_{\ell\ell} < 80$ GeV
no p_T^{miss} requirement</td><td>$m_{\ell\ell} < 55$ GeV</td><td rowspan="4">$m_{\ell\ell} < 70$ GeV

$\lvert m_{\tau\tau} - m_Z\rvert \leq 25$ GeV
central jet veto
outside lepton veto</td></tr>
<tr><td rowspan="3">$\Delta\phi_{\ell\ell} > 2.8$</td><td colspan="2">$m_{\tau\tau} > m_Z - 25$ GeV</td></tr>
<tr><td rowspan="2">$\max\left(m_T^{\ell}\right) > 50$ GeV</td><td>fail central jet veto
or fail outside lepton veto</td></tr>
<tr><td>$\lvert m_{jj} - 85\rvert > 15$ GeV
or $\Delta y_{jj} > 1.2$</td></tr>
</table>

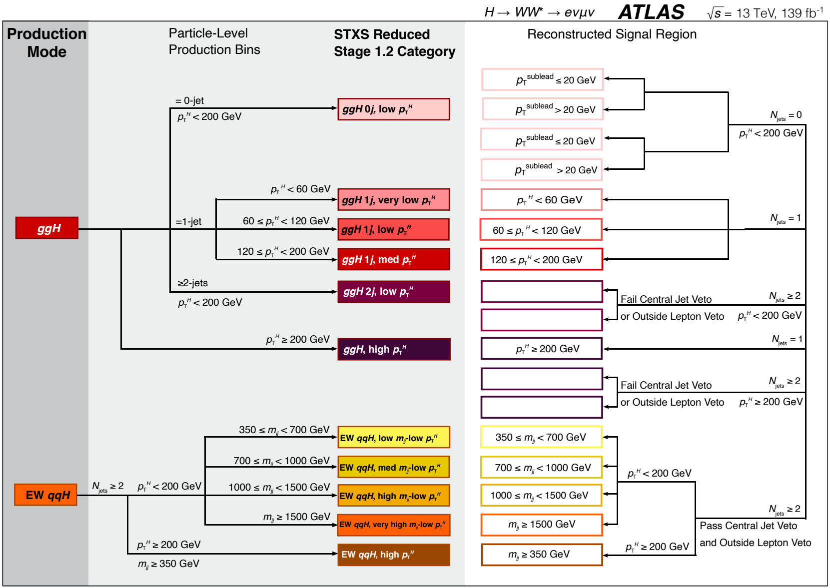
$H \to WW^* \to e\nu\mu\nu$ ATLAS $\sqrt{s}$ = 13 TeV, 139 fb^{-1}
Production Mode
Particle-Level Production Bins
STXS Reduced Stage 1.2 Category
Reconstructed Signal Region
ggH
EW qqH
= 0-jet
p_T^H < 200 GeV
=1-jet
p_T^H < 60 GeV
60 ≤ p_T^H < 120 GeV
120 ≤ p_T^H < 200 GeV
≥2-jets
p_T^H < 200 GeV
p_T^H ≥ 200 GeV
ggH 0j, low p_T^H
ggH 1j, very low p_T^H
ggH 1j, low p_T^H
ggH 1j, med p_T^H
ggH 2j, low p_T^H
ggH, high p_T^H
N_{jets} ≥ 2
p_T^H < 200 GeV
350 ≤ m_{jj} < 700 GeV
700 ≤ m_{jj} < 1000 GeV
1000 ≤ m_{jj} < 1500 GeV
m_{jj} ≥ 1500 GeV
p_T^H ≥ 200 GeV
m_{jj} ≥ 350 GeV
EW qqH, low m_{jj}-low p_T^H
EW qqH, med m_{jj}-low p_T^H
EW qqH, high m_{jj}-low p_T^H
EW qqH, very high m_{jj}-low p_T^H
EW qqH, high p_T^H
$p_T^{sublead}$ ≤ 20 GeV
$p_T^{sublead}$ > 20 GeV
$p_T^{sublead}$ ≤ 20 GeV
$p_T^{sublead}$ > 20 GeV
p_T^H < 60 GeV
60 ≤ p_T^H < 120 GeV
120 ≤ p_T^H < 200 GeV
p_T^H ≥ 200 GeV
350 ≤ m_{jj} < 700 GeV
700 ≤ m_{jj} < 1000 GeV
1000 ≤ m_{jj} < 1500 GeV
m_{jj} ≥ 1500 GeV
m_{jj} ≥ 350 GeV
N_{jets} = 0
p_T^H < 200 GeV
N_{jets} = 1
Fail Central Jet Veto
or Outside Lepton Veto
N_{jets} ≥ 2
p_T^H < 200 GeV
N_{jets} = 1
Fail Central Jet Veto
or Outside Lepton Veto
N_{jets} ≥ 2
p_T^H ≥ 200 GeV
p_T^H < 200 GeV
N_{jets} ≥ 2
Pass Central Jet Veto
and Outside Lepton Veto
p_T^H ≥ 200 GeV

Category composition in terms of STXS signals

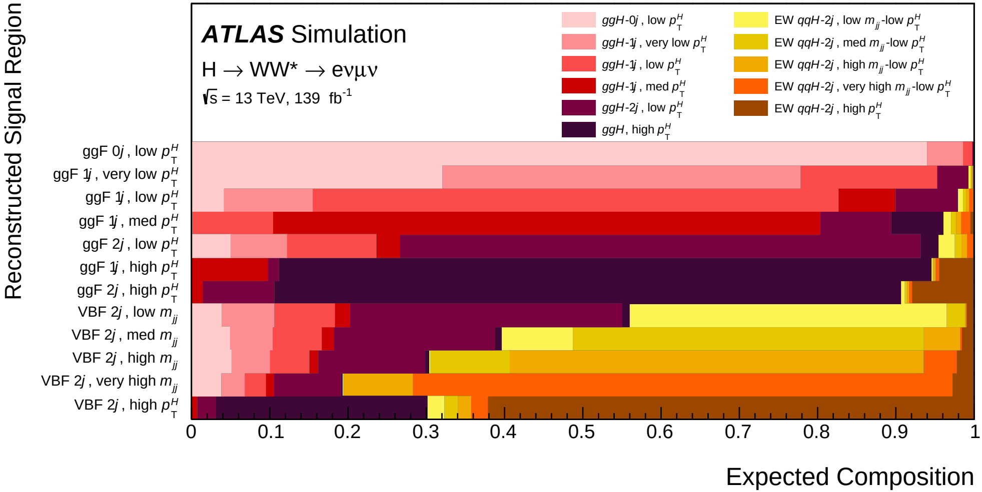

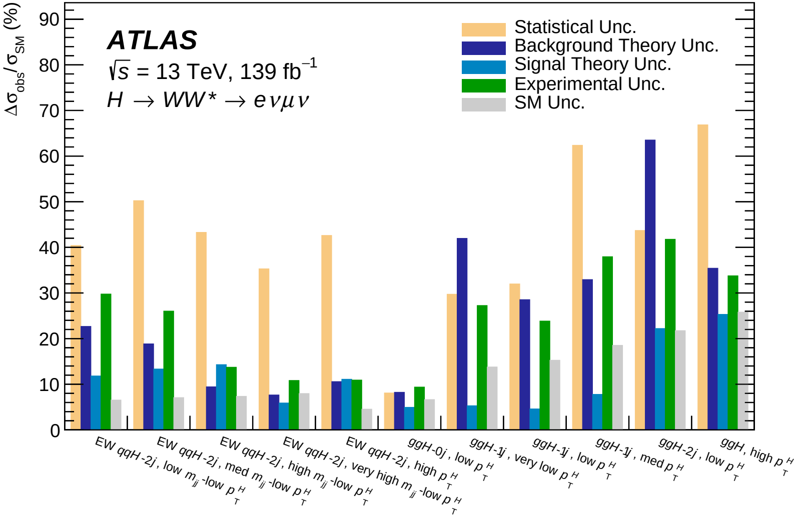
ATLAS
$\sqrt{s}$ = 13 TeV, 139 fb^{-1}
$H \to WW^* \to e\nu\mu\nu$
Statistical Unc.
Background Theory Unc.
Signal Theory Unc.
Experimental Unc.
SM Unc.
$\Delta\sigma_{obs}/\sigma_{SM}$ (%)
0
10
20
30
40
50
60
70
80
90
EW qqH-2j, low m_{jj}-low p_T^H
EW qqH-2j, med m_{jj}-low p_T^H
EW qqH-2j, high m_{jj}-low p_T^H
EW qqH-2j, very high m_{jj}-low p_T^H
EW qqH-2j, high p_T^H
ggH-0j, low p_T^H
ggH-1j, very low p_T^H
ggH-1j, low p_T^H
ggH-1j, med p_T^H
ggH-2j, low p_T^H
ggH, high p_T^H

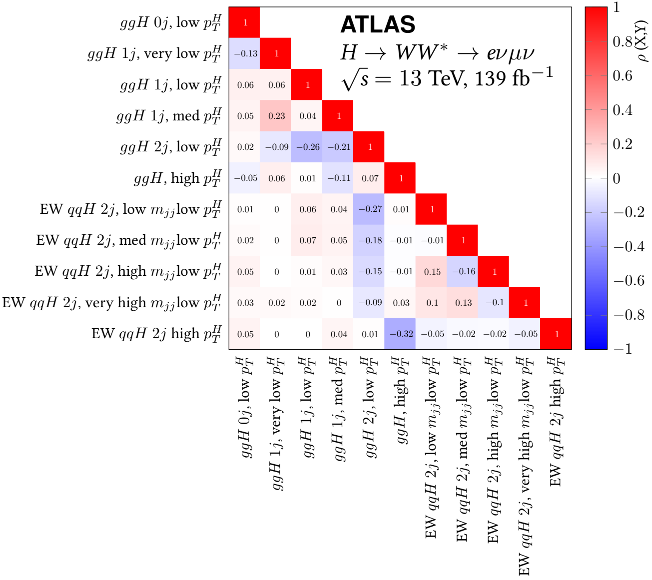
ATLAS
$H \to WW^* \to e\nu\mu\nu$
$\sqrt{s} = 13$ TeV, 139 fb^{-1}
ggH $0j$, low p_T^H
ggH $1j$, very low p_T^H
ggH $1j$, low p_T^H
ggH $1j$, med p_T^H
ggH $2j$, low p_T^H
ggH, high p_T^H
EW qqH $2j$, low m_{jj}low p_T^H
EW qqH $2j$, med m_{jj}low p_T^H
EW qqH $2j$, high m_{jj}low p_T^H
EW qqH $2j$, very high m_{jj}low p_T^H
EW qqH $2j$ high p_T^H
1
−0.13 1
0.06 0.06 1
0.05 0.23 0.04 1
0.02 −0.09 −0.26 −0.21 1
−0.05 0.06 0.01 −0.11 0.07 1
0.01 0 0.06 0.04 −0.27 0.01 1
0.02 0 0.07 0.05 −0.18 −0.01 −0.01 1
0.05 0 0.01 0.03 −0.15 −0.01 0.15 −0.16 1
0.03 0.02 0.02 0 −0.09 0.03 0.1 0.13 −0.1 1
0.05 0 0 0.04 0.01 −0.32 −0.05 −0.02 −0.02 −0.05 1
ρ(X,Y)
1
0.8
0.6
0.4
0.2
0
−0.2
−0.4
−0.6
−0.8
−1